

## Assessment of high enthalpy geothermal resources and promising areas of Chile



Diego Aravena <sup>a,b,\*</sup>, Mauricio Muñoz <sup>a,b</sup>, Diego Morata <sup>a,b</sup>, Alfredo Lahsen <sup>a,b</sup>, Miguel Ángel Parada <sup>a,b</sup>, Patrick Dobson <sup>c</sup>

<sup>a</sup> Centro de Excelencia en Geotermia de los Andes (CEGA), Facultad de Ciencias Físicas y Matemáticas, Universidad de Chile, Santiago, Chile

<sup>b</sup> Departamento de Geología, Facultad de Ciencias Físicas y Matemáticas, Universidad de Chile, Santiago, Chile

<sup>c</sup> Earth Sciences Division, Lawrence Berkeley National Laboratory, Berkeley, CA, USA

### ARTICLE INFO

#### Article history:

Received 5 March 2015

Received in revised form 15 August 2015

Accepted 2 September 2015

Available online 22 October 2015

#### Keywords:

Geothermal power potential

High enthalpy

Chilean Andes

USGS Heat in Place

Monte Carlo

### ABSTRACT

This work aims to assess geothermal power potential in identified high enthalpy geothermal areas in the Chilean Andes, based on reservoir temperature and volume. In addition, we present a set of highly favorable geothermal areas, but without enough data in order to quantify the resource. Information regarding geothermal systems was gathered and ranked to assess Indicated or Inferred resources, depending on the degree of confidence that a resource may exist as indicated by the geoscientific information available to review. Resources were estimated through the USGS Heat in Place method. A Monte Carlo approach is used to quantify variability in boundary conditions. Estimates of total Indicated resource are confined to 3 geothermal systems; Apacheta, El Tatio and Tolhuaca, yielding a total value of  $228 \pm 154$  MWe. The estimates of the total Inferred resources for Chile include 6 geothermal systems and yield a total value of  $431 \pm 321$  MWe. Standard deviation reflects the high variability of reservoir specific parameters for each system. A set of 65 favorable geothermal areas are proposed as the most likely future development targets. Eight of them have initial exploration results that suggest they are highly favorable targets as potential geothermal resources.

© 2015 Elsevier Ltd. All rights reserved.

## 1. Introduction

Early geothermal exploration in Chile began in 1921, when an Italian technical group from Larderello drilled two wells of about 70–80 m depth at El Tatio geothermal field (Tocchi, 1923). Systematic exploration resumed in 1968 as a result of a joint project by the Chilean Development Corporation (Corporación de Fomento de la Producción, CORFO) and the United Nations Development Program (UNDP) (Lahsen, 1976). In addition, geothermal exploration was carried out by the Japan International Cooperation Agency (JICA) in Puchuldiza (Lahsen, 1978; JICA, 1979; Letelier, 1981) and Surire (Cusicanqui, 1979). Since then, basic exploration, drilling and feasibility studies have been conducted sporadically, mainly by Universidad de Chile (Lahsen, 1976, 1988), the National Geological Survey (Servicio Nacional de Geología y Minería, SERNAGEOMIN) (Hauser, 1997; Pérez, 1999), and the

National Oil Company (Empresa Nacional del Petróleo, ENAP). By early 2000, a geothermal law was enacted providing the framework for the exploration and development of geothermal energy in Chile. Henceforth, comprehensive efforts to assess geothermal potential have been made by public entities and private companies (e.g. Lahsen et al., 2010 and references therein). During the first half of 2011, the Chilean Government founded the Andean Geothermal Center of Excellence (Centro de Excelencia en Geotermia de Los Andes, CEGA), a Fondap-Conicyt project hosted at the Universidad de Chile, aimed at improving geothermal knowledge and promoting its use in the Andean countries. This work is part of a nationwide geothermal evaluation carried on since then (e.g. Sánchez et al., 2011; Aravena and Lahsen, 2012, 2013).

Early resource assessments considered a gradient of  $45^{\circ}\text{C}/\text{km}$  in the Chilean Plio-Quaternary volcanic belt, yielding  $1.85 \times 10^{22}$  J of thermal energy stored in water above  $150^{\circ}\text{C}$  for depths less than 5 km (Aldrich et al., 1981). Later on, Lahsen (1986) calculated values on the order of 16,000 MWe for 50 years contained in fluids with a temperature over  $150^{\circ}\text{C}$ , and at a depth less than 3 km. Updated estimates of the geothermal potential in northern Chile yield values between 400 and 1300 MWe (Procesi, 2014). In southern Chile

\* Corresponding author at: Centro de Excelencia en Geotermia de los Andes (CEGA), Universidad de Chile, Plaza Ercilla 803, Santiago, Chile.

E-mail addresses: [daravena@ing.uchile.cl](mailto:daravena@ing.uchile.cl) (D. Aravena), [maumunoz@ing.uchile.cl](mailto:maumunoz@ing.uchile.cl) (M. Muñoz).

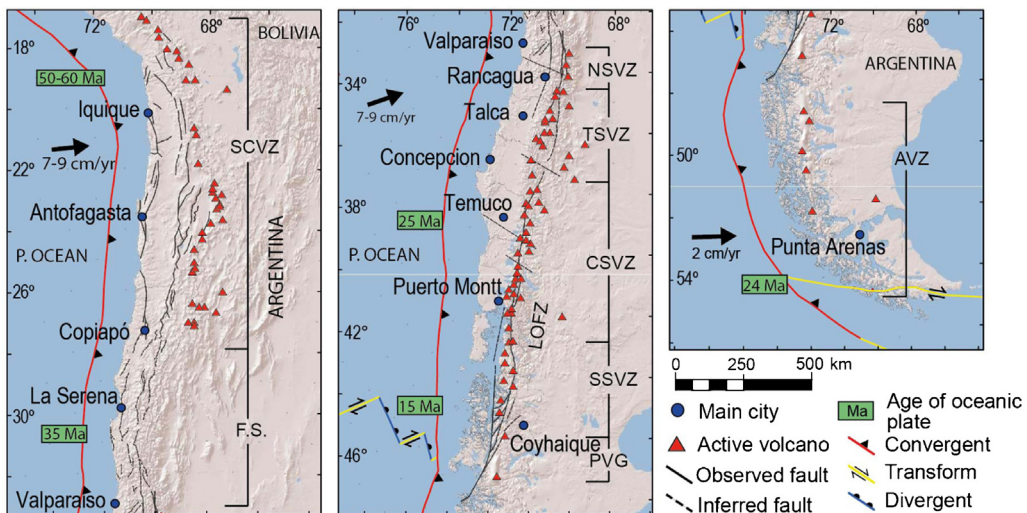


**Fig. 1.** Tectonic setting, regional scale faults and active volcanoes of the Chilean Andes. SCVZ, Southern Central Volcanic Zone; F.S., Flat Slab; NSVZ, Northernmost SVZ; TSVZ, Transitional SVZ; CSVZ, Central SVZ; SSVZ, Southern SVZ; PVG, Patagonian Volcanic Gap; AVZ, Austral Volcanic Zone. Main fault systems in the SVZ modified from Cembrano et al. (2007). Flat Slab structures modified from SERNAGEOMIN (2003). Regional structures in the SVZ modified from SERNAGEOMIN (2003), Rosenau et al. (2006), Cembrano and Lara (2009), and references therein. Age of oceanic plate after Tebbens et al. (1997).

estimates vary between 600 and 1400 MWe (Lahsen et al., 2010; Aravena and Lahsen, 2012).

This work was initiated to provide a realistic estimate of accessible geothermal resources associated with high enthalpy (>200 °C) reservoirs in the Chilean Andes, with emphasis on geological, geophysical and geochemical evidence constraining each geothermal system. To do this, we gathered and ranked published information regarding available geothermal exploration and Quaternary volcanic features to establish a hierarchy of Measured, Indicated and Inferred geothermal resources. To assess the geothermal resources of Chile, the USGS Heat in Place method is applied. Although this study does not produce absolute values of power potential, it does provide a systematic manner with which to compare prospects based on the available/published information. In addition, we present a set of areas with a favorable geothermal setting whose published information is still considered deficient.

## 2. Volcanic and geothermal setting

The Andean volcanic arc includes over 200 potentially active volcanoes, and at least 12 giant caldera/ignimbrite systems (Lee et al., 2010), occurring in four separate segments referred to as the Northern (NVZ; 2°N – 5°S), Central (CVZ; 14–28°S), Southern (SVZ; 33–46°S), and Austral (AVZ; 49–55°S) Volcanic Zones (Fig. 1). Volcanism results from subduction of the Nazca and Antarctic oceanic plates below South America (Muñoz and Stern, 1988; Cembrano et al., 2007). The country contains more than 300 geothermal areas located along the Chilean Andes, associated with Quaternary volcanism. The main geothermal systems occur in the extreme northern (17–28°S) and central-southern part (33–46°S) of Chile. In areas where Quaternary volcanism is absent, such as along the Andean volcanic gaps (28–33°S and 46–48°S), as well as in the Coastal Range, thermal springs are scarce and their temperatures are usually lower than 30 °C (Lahsen et al., 2010). The Andean volcanic arc still represents one of the largest undeveloped geothermal provinces of the world. There are currently 3 geothermal systems in the country with available measured wellhead resource values: (i) Apacheta (2 wells, 9 MWe); (ii) El Tatio (4 wells, 23 MWe); and (iii) Tolhuaca (1 well, 13 MWe). These wells yield a total confirmed power potential of 45 MWe.

## 3. Methodology

### 3.1. Selection and ranking of geothermal areas

A major challenge in geothermal resource assessment lies in quantifying the size and thermal energy of a reservoir. This work follows other Heat in Place geothermal resource studies in using the terminology adopted by Muffler et al. (1978) for the subdivision of the geothermal resource base. Geothermal resources are subdivided according to increasing geological confidence into Inferred, Indicated, and Measured categories. Areas where reservoir features have been constrained indirectly by geophysics (dimensions) and fluid geochemistry (reservoir temperature), but whose reservoir has not been reached by wells are ranked as Inferred. Areas where the reservoir has been confirmed by exploratory wells are ranked as Indicated. If the geothermal play has wells with a proven deliverability, it is ranked as Measured.

Through the analysis of geological, geochemical and geophysical data, and using a GIS weighted overlay superposition method, Aravena and Lahsen (2013) generated a nationwide map of geothermal favorability. This map, along with data gathered in this work, was used to establish two additional categories of geothermal plays: (i) highly probable resource areas for regions where geophysical surveys indicate the existence of a geothermal reservoir or fluid geothermometry suggest high temperatures associated with a deep reservoir; and (ii) interest areas for regions with extensive surface geothermal features and high temperature discharges. Interest areas include zones with discharges of lower temperature, yet whose context has a research concern, such as an unknown heat source in areas with no active volcanism (Fig. 2). Most of these areas lack available data needed to properly quantify the resource.

### 3.2. USGS Heat in Place method for reservoir constrained assessment

To assess the geothermal resources of Chile, a reformulation of the USGS Heat in Place method is applied (Garg and Combs, 2015). This model involves estimating the thermal energy available in a liquid-dominated reservoir to calculate recoverable electric power (Williams et al., 2008 and references therein). A Monte Carlo approach is used to quantify variability of boundary conditions.

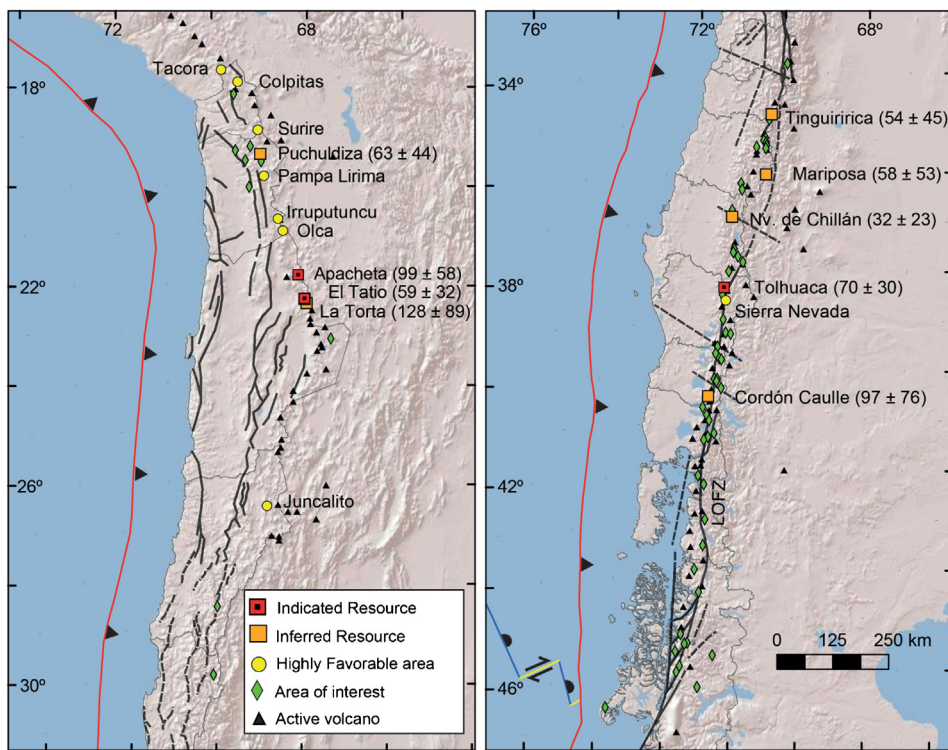


**Fig. 2.** Main geothermal areas in Chile. Indicated and Inferred resources are displayed with name and assessment results. Highly probable and interest areas are depicted in Tables 3 and 4, respectively. Regional structures as in Fig. 1.

After 100,000 iterations, the resulting power output is fitted to a probability distribution to assess the 10%, 50% and 90% confidence intervals, referred to as P90, P50 and P10, respectively. Fig. 3 shows the fit of results to a Birnbaum–Saunders distribution for the Tolhuaca geothermal system.

The USGS Heat in Place volumetric method was used in early geothermal resource estimations in the 1970s (Nathenson, 1975; White and Williams, 1975; Muffler et al., 1978; Muffler, 1979), and later improved based on updated empirical factors, and specific power cycles (e.g. Lovekin, 2004; Williams et al., 2008; Zarrouk and Moon, 2014; Garg and Combs, 2015). This method states that the electric power potential for an identified geothermal system can be determined by the reservoir thermal energy, the amount of thermal energy that can be extracted from the reservoir at the wellhead,

the specific power cycle, and the efficiency for the electric power conversion of the wellhead thermal energy (Garg and Combs, 2015 and references therein). Once mass flux and its thermal properties at the wellhead are determined, the thermodynamic and economic constraints for conversion to electric power can be calculated (e.g. DiPippo, 2012b; Zarrouk and Moon, 2014).

The reservoir thermal energy,  $q_R$  [J], is calculated as follows:

$$q_R = \bar{\rho}cV(T_R - T_r) \quad (1)$$

Here,  $\bar{\rho}c$  is the volumetric heat capacity in the reservoir [ $J/m^3 K$ ],  $V$  is the reservoir volume [ $m^3$ ],  $T_R$  is the reservoir temperature, and  $T_r$  is a reference or abandonment temperature (Garg and Combs, 2015). Regarding the reservoirs temperatures, we assessed single flash cycles for all geothermal plays. Therefore, for a single flash

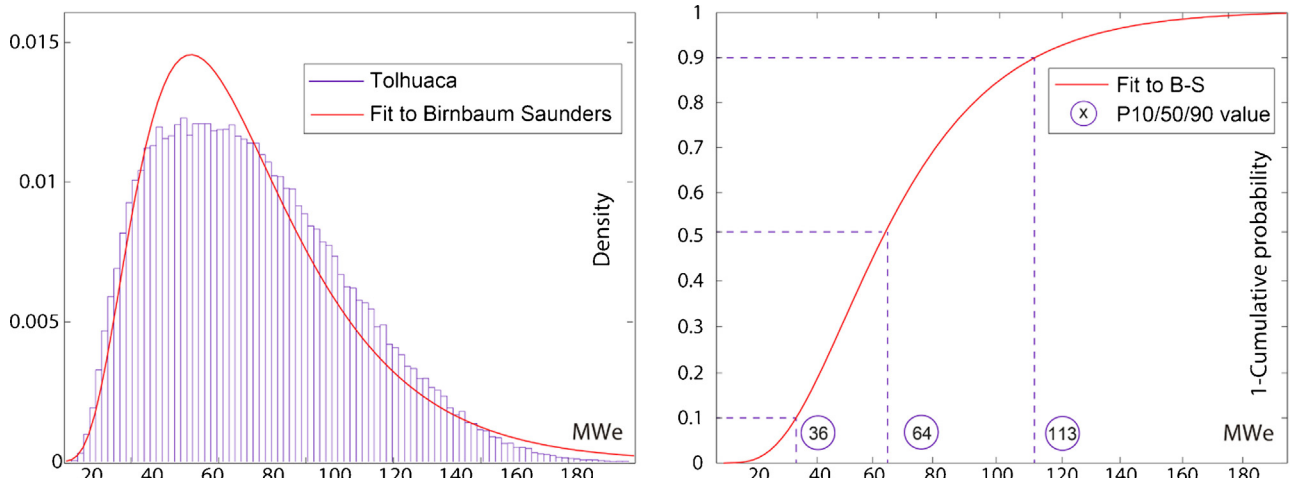


**Fig. 3.** Results after 100,000 Monte Carlo iterations for the Tolhuaca geothermal System. Left, power output results (bins) and fit (red line) to a Birnbaum–Saunders probability distribution function (PDF); right, cumulative distribution function (CDF) showing P10, P50 and P90 intervals of confidence (For interpretation of the references to color in this figure legend, the reader is referred to the web version of this article).

power plant, the abandonment temperature is given by the saturation temperature corresponding to the separator pressure (5 bar, 151.831 °C). The geothermal recovery factor  $R_g$  is defined as the ratio of the heat recovered at the wellhead  $q_w$ , to the heat stored in the reservoir  $q_R$ .

$$R_g = \frac{q_w}{q_R} \quad (2)$$

In the above equation  $R_g$  is the geothermal recovery factor [dimensionless]. Updated values of the geothermal recovery factors include 0–0.2, the latter value is believed to be the maximum reliable value based on global experience with production from liquid-dominated reservoirs (Garg and Combs, 2010). If the well drilling and testing has shown adequate well productivity, it is justified to assume a non-zero minimum value (say 0.05) for the geothermal recovery factor (Garg and Combs, 2015). In addition, we carry out a sensitivity test for the power output as a function of the geothermal recovery factor, encompassing values from the published literature.

Combining Eqs. (1) and (2), the heat recovered at the wellhead  $q_w$ , can be expressed by the following expression:

$$q_w = \alpha(T_R - T_r) \quad (3)$$

Here:

$$\alpha = R_g V \bar{\rho} c \quad (4)$$

Assuming isenthalpic flow in the wellbore and neglecting the work required to raise the water, the enthalpy of produced fluid at the well head  $h_w$ , is equal to that of liquid water at reservoir temperatures.

$$h_w = h_w(T_R) \quad (5)$$

The amount of fluid produced at the wellhead  $m_w$ , is given by:

$$m_w = \frac{q_w}{(h_w - h_r)} \quad (6)$$

Here,  $h_r$  is the enthalpy of liquid water at the reference temperature  $T_r$ . Substituting from Eq. (3) into Eq. (6), there follows:

$$m_w = \alpha \frac{(T_R - T_r)}{(h_w - h_r)} \quad (7)$$

Neglecting kinetic or potential effects, the maximum energy output per unit mass of the substance  $e$  is given by (DiPippo, 2008):

$$e = h - h_{ex} - T_{exK}(s - s_{ex}) \quad (8)$$

Here,  $h$  and  $s$  denote the enthalpy and entropy of the substance (e.g., steam) at turbine inlet conditions with temperature  $T$ ,  $T_{exK}$  is the absolute exit temperature (K), and  $s_{ex}$  is the entropy of the liquid phase (water), at the exit temperature. For mass  $m$  of substance the available work is therefore given by:

$$W_A = me = m(h - h_{ex} - T_{exK}(s - s_{ex})) \quad (9)$$

In the case of a single flash power plant, it is assumed that the produced fluid with reservoir temperature at the wellhead is separated at the separator temperature  $T_{sep}$ . The separated brine is reinjected into the reservoir, and the steam is used to generate power. The mass of the fluid produced at the wellhead is given by Eq. (7) with  $T_r = T_{sep}$ . The steam fraction of the produced fluid is:

$$m_{stm} = m_w \frac{(h_w(T_R) - h_w(T_{sep}))}{h_{gl}(T_{sep})} \quad (10)$$

Here,  $h_{gl}(T_{sep})$  denotes the heat of vaporization. Combining Eqs. (7) and (10), there follows:

$$m_{stm} = \alpha \frac{(T_R - T_{sep})}{h_{gl}(T_{sep})} \quad (11)$$

Substituting  $m_{stm}$  for  $m$  in Eq. (9), the available work for the single flash case is given by:

$$W_{A\text{flash}} = \alpha \frac{(T_R - T_{sep})}{h_{gl}(T_{sep})} (h_{stm}(T_{sep}) - h_w(T_c) - T_{ck}(s_{stm}(T_{sep}) - s_w(T_c))) \quad (12)$$

In the above equation,  $T_c$  denotes the condenser temperature (assumed to be 40 °C; Garg and Combs, 2015), and  $T_{ck}$  is the absolute condenser temperature.

A conservative value for the electrical conversion efficiency  $\eta_u$  of 70–80% is proposed by Garg and Combs (2015), thus we used 75% for calculations. In addition, a load factor  $f_{load}$  of 0.95 is considered. Therefore, the electric power for a given period of years is determined as follows:

$$W_e = \frac{W_{A\text{flash}} \eta_u}{Y f_{load}} \quad (13)$$

Finally, for calculation simplicity, the years ( $Y$ ) in Eq. (13) are expressed in seconds [s].

## 4. Results

### 4.1. Inferred and Indicated resources

#### 4.1.1. Boundary conditions

Parameters required for the calculation are summarized in Table 1. Reservoir specific parameters must be established individually for each geothermal system since they constrain the geometry and temperature/enthalpy of the Indicated or Inferred reservoir. Common parameters remain constant for all systems. For instance, for the Tolhuaca geothermal prospect, reservoir specific parameters were extracted from the geological setting and geothermal surveys performed in the area (Table 1).

Variability in the estimates is accommodated through a Monte Carlo simulation approach. For each system, we determine most likely (m.l.), minimum (min) and maximum (max) values for reservoir temperature, thickness, and area. Those values are used to generate triangular (min, m.l. and max) and uniform (min, max) probability distributions. Parameters with only a most likely value (m.l.) remain constant for each Monte Carlo iteration (Table 1).

#### 4.1.2. Geological, geochemical and geophysical constraints

We considered 9 geothermal prospects that have enough information to estimate their power potential. The first three systems presented below are ranked as Indicated (Apacheta, El Tatio

**Table 1**

Parameters required for the calculation of the electric generation capacity using the USGS volumetric Heat in Place method for the Tolhuaca geothermal system. Constraints are shown as Minimum (min), most likely (m.l.) and maximum (max) values for reservoir specific and common parameters.

Reservoir specific parameters	min	m.l.	max
Area (km <sup>2</sup> )	4	–	8
Thickness (km)	1	–	1.4
Temperature (°C)	250	280	300
USGS Heat in Place parameters			
Volumetric heat capacity (kJ/m <sup>3</sup> K)	–	2700	–
Abandonment temperature (°C)	–	151.831	–
<sup>a</sup> Geothermal recovery factor (%)	0	–	20
Condenser temperature (°C)	–	40	–
Electric conversion efficiency (%)	–	75	–
Plant load factor (%)	–	95	–
Plant or project life (years)	–	30	–

<sup>a</sup> For Indicated geothermal resources, which have well drilling and testing confirming the presence of a geothermal resource, the minimum geothermal recovery factor value is set at 5%.

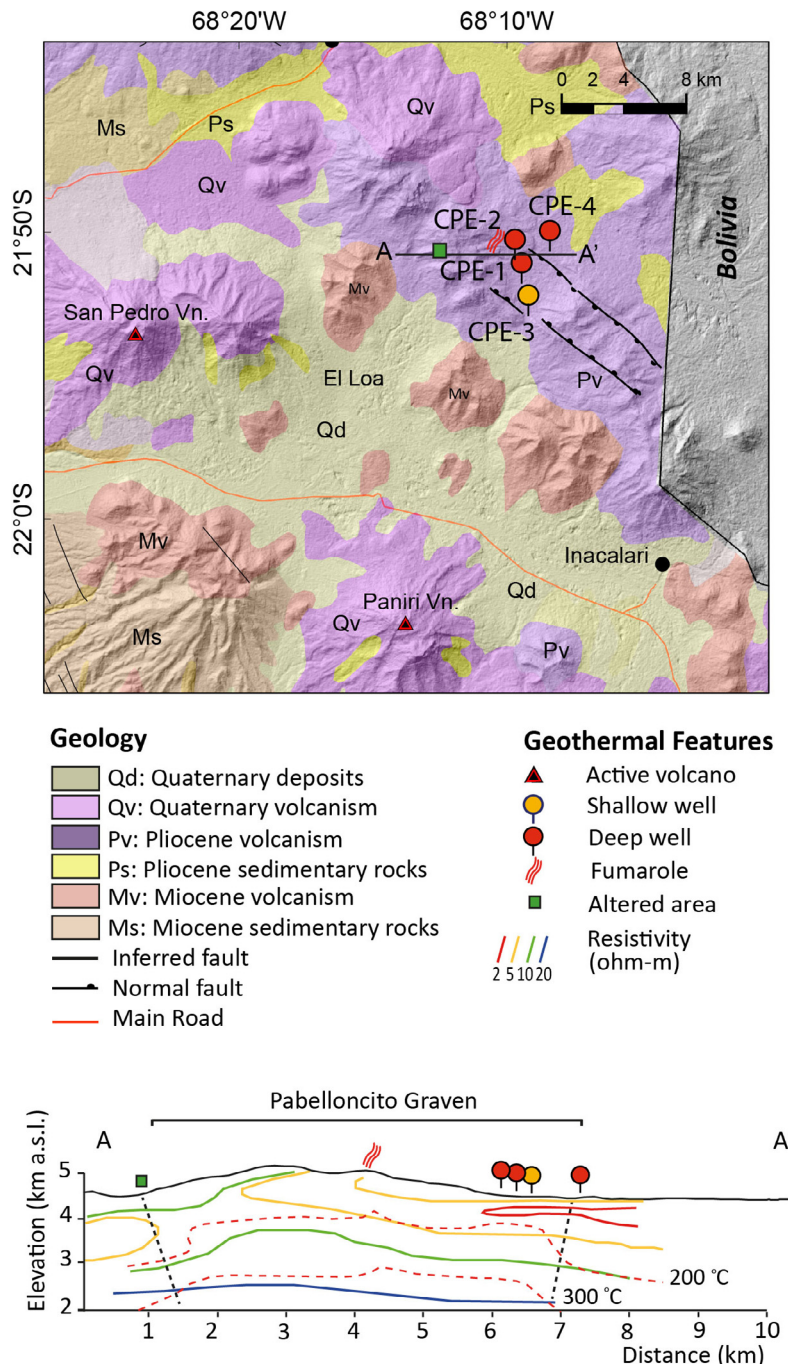


**Fig. 4.** Geological map of the Apacheta area. Geology modified from Ramírez and Huete (1981). Bottom; schematic cross section with geothermal features and well location. Projected faults, MT and temperature interpretation modified from Urzua et al. (2002).

and Tolhuaca). The remaining 6 systems are ranked as Inferred (Puchuldiza, La Torta, Tinguiririca, Mariposa, Nevados de Chillán, and Cordón Caulle). El Tatio/La Torta is considered as two separate systems even though they probably share a deep reservoir (see details in text).

#### Apacheta/Cerro Pabellón geothermal system

The Cerro Pabellón geothermal power generation project, located in the Apacheta geothermal concession in Antofagasta region, Chile, is owned by a joint project between Enel Latin-American (Chile) Ltd., and the National Oil Company (ENAP). The project, already approved by the environmental authorities and currently under development, involves the construction and operation of a geothermal power plant with an installed capacity of

48 MWe (ENEL, 2012). This graben-hosted system has four deep wells, placing it into the Indicated Resource category. The thickness of the reservoir is constrained by the convective regime in wells CPE-1 (880 m) and CPE-2 (1120 m), starting at 900 and 820 m depth, respectively. Wells CPE-4 and CPE-3 show a conductive regime (ENEL, 2012). Horizontal extension of the reservoir will be assessed as parallel and perpendicular to the graben, following the conceptual model proposed by Urzua et al. (2002) (Fig. 4). The minimum horizontal extension of the reservoir is given by the distance between wells (4 km<sup>2</sup>). Maximum extension in the NE-SW orientation is given by the projected distance between the graben main faults at the depth of the reservoir. In the NW-SE direction, maximum extension will be considered as the linear projection of

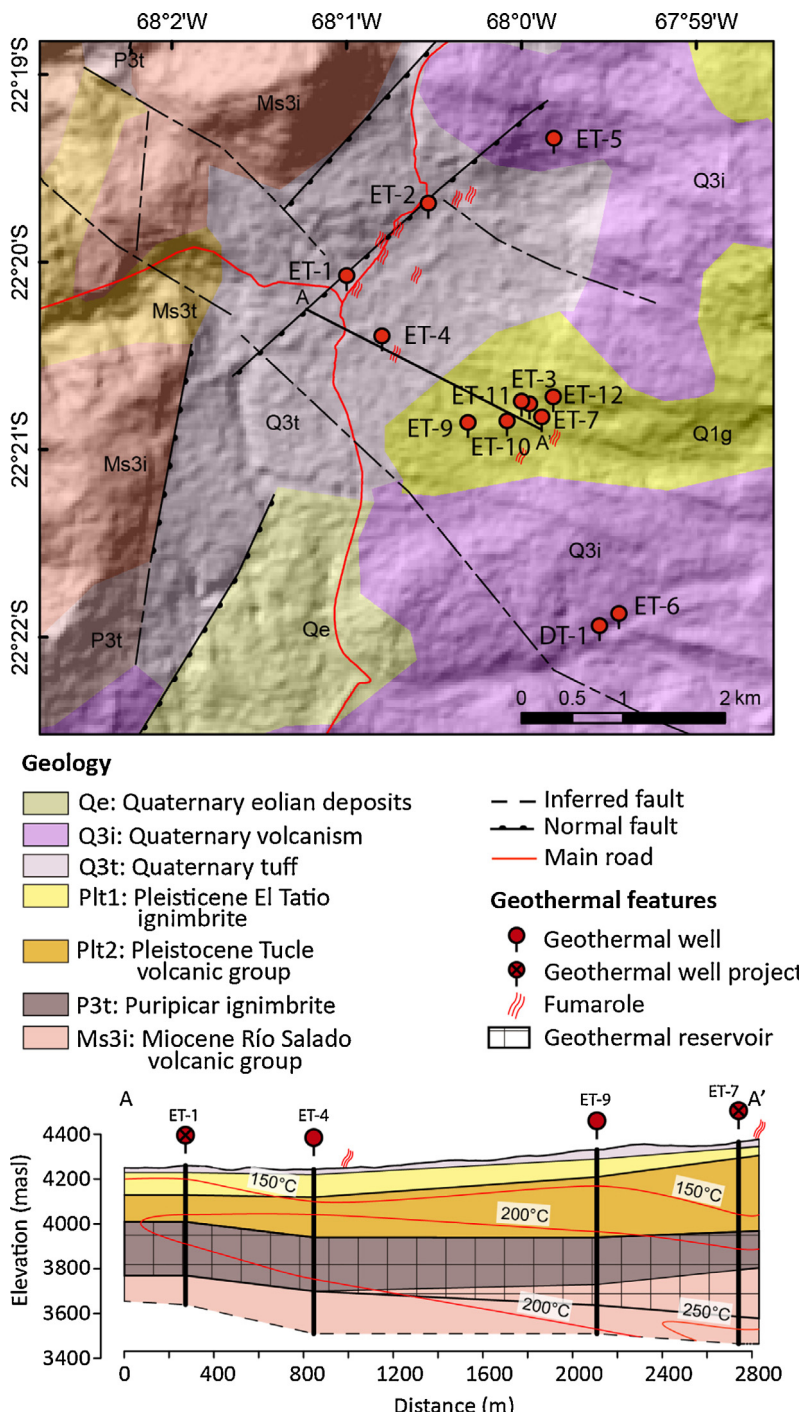


**Fig. 5.** Geological map of El Tatio area. Borehole data from Lahn and Trujillo (1976), Sarmiento et al. (2010). Bottom: geological cross section with geothermal features and well location.

thickness vs distance for wells CPE-1 and CPE-2 ( $\sim 5 \times 5 \text{ km}^2$ ). Minimum and maximum temperatures of the reservoir are reached in wells CPE-2 (212 °C) and CPE-1 (256 °C), consistent with gas geothermometry estimates of around 250 °C reported by Urzua et al. (2002).

#### El Tatio/La Torta geothermal system

The El Tatio geothermal prospect is one of the largest geothermal fields of South America (Fig. 5). This geothermal system comprises 85 fumaroles, 62 hot springs, 40 geysers, 5 mud volcanoes and extensive sinter terraces, scattered over an area of 30 km<sup>2</sup> (Tassi et al., 2005). The La Torta geothermal field is located at the southern

extension of the eastern edge of the El Tatio graben. Geophysical evidence suggests that El Tatio and La Torta share the same deep reservoir. According to the interpreted resistivity structure, the El Tatio geothermal system must be at the edge (out-flow) of the main geothermal reservoir located in the La Torta prospect, which contains the main up-flow zone (Cumming et al., 2002). We use a conservative approach, assessing the areas as separate reservoirs with different constraints and resource categories.

The geometry of the El Tatio reservoir is constrained by exploratory and exploitation wells, and therefore qualifies as an Indicated system. The minimum and maximum reservoir thickness

is 150 m and 600 m, respectively, as constrained by well data (Lahsen and Trujillo, 1976; Sarmiento et al., 2010). The average thickness of the Puripicar and Río Salado ignimbrite is 430 m, considered as the most likely value (Lahsen and Trujillo, 1976). Minimum resource area ( $11.5 \text{ km}^2$ ) is constrained by wells where convective heat transfer zones are observed, and the maximum areal extent is constrained by early geophysical surveys, where  $30 \text{ km}^2$  was estimated through vertical electrical sounding interpretation (Lahsen and Trujillo, 1976). A minimum temperature of  $213^\circ\text{C}$  was measured in well 8 and the maximum temperature of  $260^\circ\text{C}$  was encountered in well 7 (Lahsen and Trujillo, 1976); these values are selected as the minimum and maximum reservoir temperatures, respectively. A most likely value of  $250^\circ\text{C}$  was selected for calculations.

The main reservoir at the La Torta prospect was constrained by geochemical and geophysical evidence. Cumming et al. (2002) delineate a  $20 \text{ km}^2$  low resistivity anomaly ( $<10 \Omega\text{m}$ ) under the El Tatio volcanic chain. This value will be considered as the most likely, with a variability of  $5 \text{ km}^2$ , therefore a minimum areal extent of  $15 \text{ km}^2$  and a maximum of  $25 \text{ km}^2$  were considered. Minimum thickness is 650 m, based on well data (Sarmiento et al., 2010). Maximum thickness can reach 2000 m based on stratigraphic data and MT survey results (Cumming et al., 2002). The minimum temperature is  $240^\circ\text{C}$ , based on temperatures reached by wells located on the southern edge of the El Tatio prospect. The maximum temperature is constrained by gas geothermometry which suggests that the temperatures in the El Tatio-La Torta deep geothermal reservoir reaches up to  $270^\circ\text{C}$  (Tassi et al., 2010).

#### Tolhuaca geothermal system

The Tolhuaca geothermal system was confirmed by a flow test of one of the deep wells, and thus can be considered as an indicated resource. As proposed by Melosh et al. (2012), we consider a two level reservoir with steam and steam-heated waters at shallow depths, and a deep liquid reservoir below. For simplicity, they will be treated as individual reservoirs in closed systems. Between 200 and 600 m depth, temperatures in Tol-2 are above the hydrostatic 1.1 wt% gas boiling point for depth (BPD) curve, suggesting steam-dominated conditions nearby; similar conditions were encountered in Tol-1 between 200 and 400 m depth, consistent with a convective thermal regime (Melosh et al., 2012). Most wells reach  $150\text{--}200^\circ\text{C}$  at 500 m depth (considered as min. and max. respectively). The results for the shallow reservoir show power production values of less than 1 MWe, and therefore are not considered as commercial when compared to the deep reservoir. The deep well, Tol-3, encountered a liquid-dominated reservoir from 1100 to 2500 m depth at  $300^\circ\text{C}$ , consistent with the high temperature propylitic alteration zone ( $>250^\circ\text{C}$ ) observed in the other wells (Iriarte, 2013, Fig. 6). These values will be used as the maximum thickness and temperature respectively. The minimum horizontal extent of the reservoir is constrained by a low resistivity conductive anomaly associated with a  $7\text{--}8 \text{ km}^2$  clay cap, identified by Melosh et al. (2012).

#### Puchuldiza geothermal system

The Puchuldiza geothermal prospect is characterized by extensive superficial geothermal features such as thermal springs, fumaroles and mineral alteration (Tassi et al., 2010). The minimum areal extent is  $10 \text{ km}^2$  which is delineated by shallow exploratory wells ( $<600 \text{ m}$  deep, reaching  $170^\circ\text{C}$ ). Vertical electrical soundings indicate a potential maximum areal extent of  $28 \text{ km}^2$  (JICA, 1979; Lahsen et al., 2010). Geological and geophysical surveys indicate a reservoir thickness ranging between 600–1000 m (Ortiz et al., 2008 and references therein). A minimum reservoir temperature of  $200^\circ\text{C}$  was measured in a 1000 m deep exploratory well, whereas the most likely and maximum reservoir temperature is expected to reach  $250^\circ\text{C}$  and  $270^\circ\text{C}$ , respectively, based on Na-K and Na-K-Ca geothermometry (Ortiz et al., 2008).

#### Tinguiririca geothermal system

The Tinguiririca geothermal project is located  $\sim 150 \text{ km}$  SW of Santiago within the main Andean Range, on the western flank of the Tinguiririca Volcanic Complex. The Tinguiririca reservoir volume is constrained by the potential up-flow zone identified by Clavero et al. (2011), a subtle concave shaped conductive anomaly at 2500 m.a.s.l interpreted by Lira (2011) as a deep geothermal reservoir, although this preliminary conclusion is subject to further exploration. This surface covers between 5 and  $25 \text{ km}^2$ ; the minimum and maximum thickness of the reservoir are 500 m and 1000 m, respectively, accounting for the distance between the 10–75 and 10–120 ( $\Omega\text{m}$ ) intervals respectively ( $<10 \Omega\text{m}$  is interpreted to be a low resistivity clay altered cap). The lower temperature of the reservoir is given by the temperature reached in well Pte-1,  $210^\circ\text{C}$ . The maximum temperature is estimated to be  $300^\circ\text{C}$ , based on geothermometry by Clavero et al. (2011), Vázquez et al. (2014).

#### Mariposa geothermal system

The Mariposa Geothermal System (MGS) is located  $\sim 300 \text{ km}$  south of Santiago in the TSVZ. It lies within an area characterized by extensive Quaternary volcanism associated with the Maule Volcanic Complex and the Tatara-San Pedro-Pellado volcanic complex. A volumetric resource assessment performed by SKM yielded 320 MWe for a plant life of 30 years. In this assessment, the reservoir area was constrained by a  $23 \text{ to } 27 \text{ km}^2$  conductive anomaly obtained during the 2009 and 2010 MT surveys (Hickson et al., 2011). In this case we consider a minimum value of  $9 \text{ km}^2$ , accounting for the two principal upflow areas inferred by Hickson et al. (2011), this value can be extended to a less conservative  $23 \text{ km}^2$  as interpreted from data presented by Hickson et al. (2011). Reservoir thickness is taken from the base of the conductor (600–1000 m depth) to a depth that can be readily accessed by drilling, and up to the thickness of the Oligocene-Miocene units that host the reservoir, yielding values ranging from 1 to 2 km thick. The minimum reservoir temperature is constrained by the well MP-1 ( $210^\circ\text{C}$ ), maximum temperature ( $300^\circ\text{C}$ ) is based on gas geothermometry by Hickson et al. (2011).

#### Nevados de Chillán geothermal system

The Nevados de Chillán geothermal area is associated with a 13 km long NW trending volcanic chain comprising calderas, polygenetic volcanoes and flank volcanoes. Hot springs discharge over 500 l/s of sulfate-bicarbonate waters with temperatures of up to  $70^\circ\text{C}$ , equal to a heat loss of about 100 MWt (Sepúlveda and Lahsen, 2003). The reservoir volume is constrained by a concave shaped resistivity anomaly interpreted from an MT survey performed by the National Geothermal Company (Empresa Nacional de Geotermia, ENG) (ENG, 2007). The size of the anomaly ranges from 6 to  $15 \text{ km}^2$ . The reservoir has an estimated thickness varying from 500 to 1000 m, with minimum and maximum temperatures of  $220^\circ\text{C}$  and  $260^\circ\text{C}$ , based on temperatures reached by well Nieblas-1 and gas geothermometry respectively (ENG, 2007). The shallow reservoir reached by NCh-1 is considered too small for electric generation and therefore will not be included in the assessment.

#### Cordón Caulle geothermal system

The Cordón Caulle geothermal area is located in a 15 km long, 5 km wide, flat-topped volcano-tectonic depression, bounded to the northwest by the 8.5 km wide caldera of the Cordillera Nevada, and to the southeast by the 2240 m high Puyehue volcano (Sepúlveda et al., 2007 and references therein). The minimum reservoir area is inferred from the distribution of thermal springs,  $\sim 8 \text{ km}^2$ , on the other hand the maximum area may be expanded to  $20 \text{ km}^2$ , as suggested by gravity and MT data (Sepúlveda, 2005; Rojas, 2013). Based on stratigraphic relationships, gravity, MT, and seismic data, the thickness for the potential reservoir was estimated between 500 and 2000 m (Sepúlveda, 2005; Rojas, 2013). Gas geothermometry yields temperatures from 240 to  $300^\circ\text{C}$  (Sepúlveda et al., 2007).

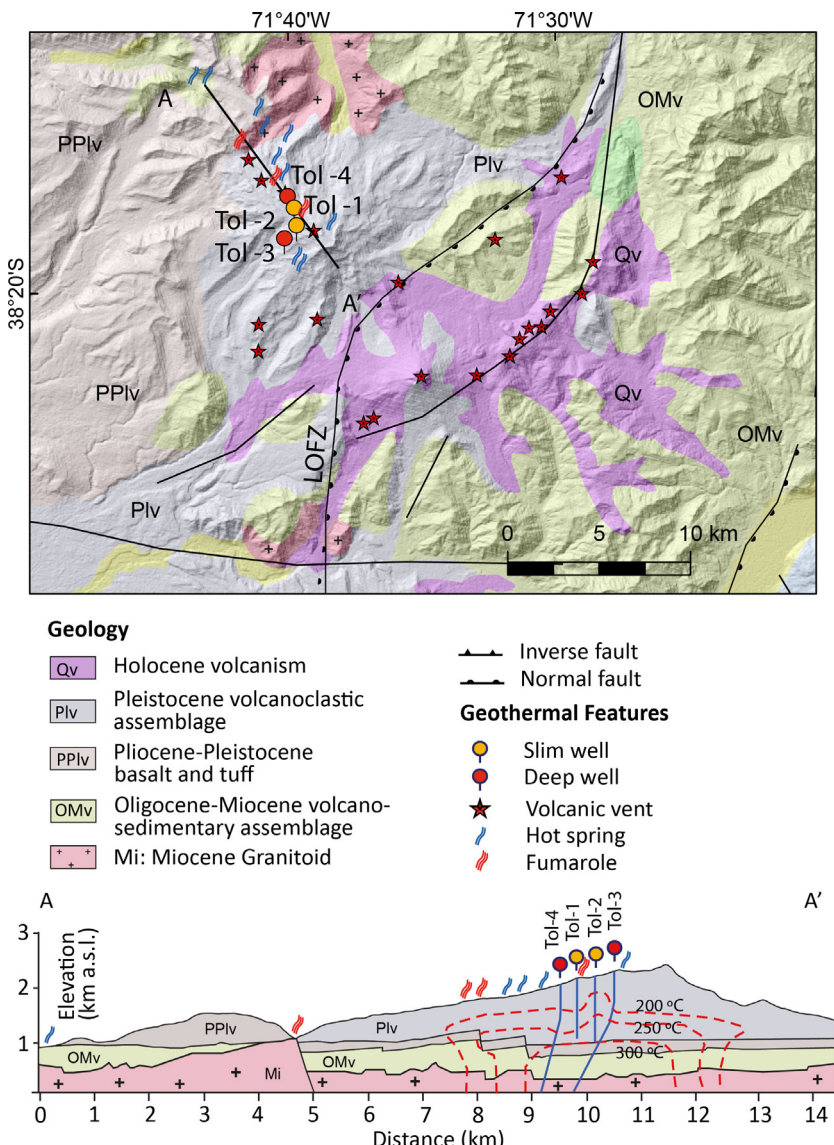


**Fig. 6.** Geological map of Tolhuaca area (modified from Emparán et al., 1997; SERNAGEOMIN, 2003; Rojas et al., 2014) including Quaternary volcanic vents (modified from Moreno et al., 1989) and main structures (Rosenau et al., 2006; Peréz et al., 2012 and references within); Geographic coordinates WGS84, zone 19°S. Bottom: Schematic cross section with geothermal features, wells and temperature interpretation after Iríarte (2013). LOFZ, Liquiñe Ofqui Fault Zone.

#### 4.1.3. Inferred and Indicated resource

Results for the Heat in Place method are summarized in Table 2, along with the standard deviation, and probability confidence intervals of 10, 50 and 90%. The Heat in Place method yields a total mean estimate of 659 MWe distributed among the 9 geothermal systems, with a mean standard deviation of 49 MWe. The three Indicated systems yield a total value of 119 MWe with a standard deviation of 154 MWe. Of these systems, Apacheta and Tolhuaca are estimated to reach 99 and 70 MWe respectively. On the other hand, El Tatio yields only 56 MWe, because of its low reservoir thickness. La Torta, and Cordón Caulle have the highest estimated power output with Inferred category, reaching 128, and 97 MWe, respectively. The remaining systems, Puchuldiza, Tinguiririca, Mariposa (Laguna Del Maule), and Nevados de Chillán, yield intermediate values of 63, 54, 58, and 32 MWe, respectively (Table 2).

#### 4.2. Highly probable resource areas

Geothermal plays where geophysical surveys indicate the existence of a geothermal reservoir, or geothermometry suggests

high temperature associated with a deep reservoir are ranked as highly probable resource areas (Table 3). Each geothermal play is described below.

##### Tacora

The Tacora geothermal prospect is associated with the 5980 m high volcano with the same name close to the Chile-Peru international boundary. This geothermal prospect is characterized by intense fumarolic activity and with extensive, white colored, superficial alteration areas along the NW and W flanks of the volcanic structure. Chemical and isotopic compositions of the main carbon species are interpreted to indicate the presence a deep geothermal reservoir with temperatures of 270–310 °C (Capaccioni et al., 2011).

##### Colpitas

The Colpitas geothermal prospect is located in the northernmost part of Chile in the Arica and Parinacota region. The area is characterized by volcano-sedimentary sequences ranging in age from Miocene to Holocene, with at least 3 nearby active volcanoes. Thermal springs are located at the bottom of a wide basin, with spring water temperatures ranging from 28 to 55 °C and a total discharge of 10 l/s. Na/K geothermometry suggests equilibration

**Table 2**

Geothermal systems selected for the assessment of Indicated and Inferred Resource.

System	Location		Area	Thickness	Temperature	Results [MWe]		Fit to distribution [MWe]		
	Name	Lat. S	Long. W	km <sup>2</sup>	m	°C	Mean	Std	P10	P50
<sup>a</sup> Apacheta	21.84	68.15	4–25	880–1120	212–250–256	99	58	185	81	72
<sup>a</sup> El Tatio	22.33	68.01	11.5–30	150–430–650	213–250–260	59	32	105	51	25
<sup>a</sup> Tolhuaca	38.31	71.66	4–8	1000–1400	250–280–300	70	30	110	69	33
<sup>b</sup> Puchuldiza	19.41	68.98	10–28	600–1000	200–250–270	63	44	127	52	13
<sup>b</sup> La Torta	22.42	67.97	15–25	650–2000	240–270	128	89	256	107	27
<sup>b</sup> Tinguiririca	34.85	70.38	5–25	500–1000	210–300	54	45	117	42	9
<sup>b</sup> Mariposa	36.06	70.53	9–23	500–1000	210–300	58	43	120	47	11
<sup>b</sup> Nv. de Chillán	36.90	71.40	6–15	500–1000	220–260	32	23	66	27	7
<sup>b</sup> Cordón Caulle	40.49	72.16	8–20	500–2000	240–300	97	76	203	77	17
Total						659	439	1290	548	180

Categories:

<sup>a</sup> Indicated.<sup>b</sup> Inferred.

Minimum, most likely and maximum values for the area, thickness and temperature of the reservoir are included. Mean electrical power output (MWe), standard deviation after 100,000 Monte Carlo iterations and 10–50–90% confidence interval after fitting the results to Birnbaum Saunders (Indicated) and Weibull (Inferred) probability distribution. Geographic coordinates WGS84, zone 18–19°S.

**Table 3**

Highly probable resource areas and geothermal related surveys in the Chilean Andes. Geographic coordinates WGS84 zones 18–19°S. 1. Cusicanqui (1979); 2. De Silva et al. (1991); 3. González-Ferrán (1995); 4. Tassi et al. (2010); 5. Aguirre et al. (2011); 6. Arcos et al. (2011); 7. Capaccioni et al. (2011); 8. Muñoz et al. (2011); 9. Reyes et al. (2011); 10. Risacher et al. (2011); 11. Tassi et al. (2011); 12. Legault et al. (2012); 13. García (2014)

Name	Lat. S	Lon. W	Survey	Ref.
Tacora	17.70	69.80	Chemical and isotopic assessment of gas emissions.	1
Colpitas	17.95	69.45	3-D MT geophysical survey; Chemical assessment of hot water discharges.	5
Surire	18.92	68.06	Chemical and isotopic assessment of gas emissions and water discharges.	1, 4, 10
Pampa Lirima	19.85	68.90	Geophysical survey; water and gas geothermometry; Exploratory wells.	4, 6, 12
Irruputuncu	20.71	68.59	MT, TDEM and ZTEM geophysical surveys; Chemical and isotopic assessment of gas emissions and water discharges.	9, 11
Olca	20.95	68.48	Geophysical survey; Chemical and isotopic assessment of gas emissions and water discharges.	1, 2, 3, 11
Juncalito	26.51	68.82	Geophysical survey; gas geothermometry; exploratory wells.	10, 13
Sierra Nevada	38.57	71.62	Geophysical survey; shallow exploratory wells.	8

temperatures higher than 200 °C. A 3-D MT study shows a conductive area (3–8 Ωm) of several tens of km<sup>2</sup> interpreted as the clay cap of an inferred geothermal reservoir (Aguirre et al., 2011).

#### Surire

The Surire geothermal prospect is located south of the Surire salt deposits near the Polloquere volcano. Conventional aqueous geothermometers cannot be used because of the salt deposits (Risacher et al., 2011). Nevertheless, silica geothermometry indicates equilibrium temperatures ranging from 150 to 180 °C (Cusicanqui, 1979). The gas composition indicates medium to high equilibrium temperatures (>200 °C), suggesting interactions of deeply circulating and shallow waters (Tassi et al., 2010).

#### Pampa Lirima

The Pampa Lirima geothermal project is located in the Altiplano of northern Chile, within the Central Andes Volcanic chain. The geochemical features of thermal water and gas discharges at Pampa Lirima are typical of fluids that have evolved within shallow aquifers; therefore low temperature aquifers may mask any signal of deep fluids (Tassi et al., 2010; Achurra, 2011). An MT/TDEM geophysical survey was carried out at Pampa Lirima, revealing a large conductive anomaly interpreted as a deep geothermal reservoir (Arcos et al., 2011), although this preliminary conclusion is subject to further exploration. In addition, ZTEM inversion images appear to agree very well with the MT data, including the presence of a conductive layer at >500 m below the Pampa Lirima valley (Legault et al., 2012).

#### Irruputuncu

Irruputuncu is a geothermal prospect located near the southeastern edge of the Tarapacá region, in northern Chile, east of the Doña Ines de Collahuasi copper mine, the owner of the geothermal exploration concession. Acid sulphate hot springs discharge at the base of the Irruputuncu dacitic stratovolcano (Reyes et al., 2011).

A 3-D inversion of TEM-MT data indicates two conductive layers separated by a resistive zone. Beneath the conductive layers lies a resistive structure, interpreted as a high temperature geothermal reservoir (Reyes et al., 2011). Two slim holes drilled west of the Irruputuncu volcano (800 and 1430 m depth) encountered bottom hole temperatures of 150 °C and 195 °C (at 3350 and 3000 m.a.s.l., respectively) and record an argillic alteration assemblage. Temperature profiles were conductive and TEM-MT data suggests a potential deep reservoir temperature up to 220 °C (Reyes et al., 2011).

#### Olca

The Olca stratovolcano forms part of a 20 km long, EW-oriented volcanic chain that includes Paruma and Michincha volcanoes (De Silva et al., 1991; González-Ferrán, 1995). The Olca geothermal prospect is characterized by a scarcity of superficial manifestations, as fumaroles are only found at the volcano crater, and a single warm spring is located at the base of the volcano. Groundwater exploration wells (<700 m) drilled at the base of the Olca volcano revealed an extensive clay-cap and temperatures up to 70 °C. Beneath this clay-cap, there is a high resistivity zone interpreted to result from high temperature alteration in the geothermal reservoir (Reyes et al., 2011). He, δ<sup>18</sup>O and δD isotopic signatures of the fumaroles suggests a mixing process between magmatic and hydrothermal sources. Gas geothermometry suggests equilibrium temperatures of 280–400 °C (Tassi et al., 2011).

#### Juncalito geothermal area

The Juncalito geothermal prospect is located in the Claudio Gay Cordillera, at the southern end of the CVZ, between eroded Miocene volcanic centers to the west, and Pliocene to Holocene volcanic centers to the east. An MT survey performed in 2012 shows a 2 km thick low resistivity anomaly, interpreted as the clay cap (<16 Ωm) above an inferred geothermal reservoir (~100 Ωm). The geology

**Table 4**

Interest Area locations and geothermal features in the Chilean Andes. References in right column. Geographic coordinates WGS84 zones 18—19°S. 1 [Días \(1983\)](#); 2 [Hauser \(1989\)](#); 3 [Hauser \(1997\)](#); 4 [Peréz \(1999\)](#); 5 [Risacher et al. \(2011\)](#)

Name	Lat. S	Long. W	Geothermal feature	Ref.
Jurase	18.20	69.53	Hot springs temperature 65 °C; hydrothermal alteration; and silica sinters	1, 3, 5
Berenguela	19.25	69.18	Hot springs temperature 58 °C	1, 3
Quitatiri	19.34	69.50	Hot springs temperature 87 °C	1, 3
Chimisa	19.38	69.29	Hot springs temperature 90 °C	1, 3, 5
Laguna Churicollo	19.55	68.95	Hot springs temperature 90 °C	1, 3
Mamiña	20.07	69.21	Hot springs temperature 52 °C	1, 3, 5
Aguas Calientes	23.13	67.43	Hot springs temperature 50 °C	1, 3, 5
El Toro	29.91	70.05	Hot springs temperature 60 °C	1, 3
Colina	33.83	69.98	Hot springs temperature 50 °C	3
Termas del Flaco	34.95	70.43	Hot springs temperature 77 °C	3
El Azufre	35.32	70.54	Hot springs temperature 70 °C	3
El Llollí	35.37	70.58	Hot springs temperature 95 °C	3
El Colorado	35.41	70.52	Hot springs temperature 75 °C	3
Tigre Naciente	35.47	70.51	Hot springs temperature 65 °C	3
Estero El Volcán	35.50	70.76	Hot springs temperature 95 °C	3
Descabezado Chico	35.53	70.54	Hot springs temperature 80 °C	3
Baños de la Turbia	36.29	71.17	Hot springs temperature 50 °C	3
Baños de Longaví	36.35	71.14	Hot springs temperature 81 °C	3
San Lorenzo	36.76	71.40	Hot springs temperature 60 °C	3
Aillin	37.54	71.38	Hot springs temperature 93 °C; extensive hydrothermal alteration	3
Quilaquín	37.60	71.40	Hot springs temperature 75 °C	3
Emanuel	37.60	71.28	Hot springs temperature 54 °C	3
Copahue	37.82	71.16	Hot springs temperature 93 °C	3
Avellano	37.99	71.53	Hot springs temperature 81 °C	3, 5
Manzanar	38.46	71.71	Hot springs temperature 52 °C	3, 5
Balboa	38.96	71.71	Hot springs temperature 67 °C	3, 5
Huife	39.22	71.66	Hot springs temperature 60 °C	3
Panqui	39.25	71.53	Hot springs temperature 50 °C	3
Geométricas	39.50	71.87	Hot springs temperature 72 °C	3, 4, 5
Coñaripe	39.63	71.92	Hot springs temperature 62 °C	3, 4
Liquiñe	39.74	71.84	Hot springs temperature 82 °C	3, 4
Hipólito Muñoz	39.76	71.79	Hot springs temperature 85 °C	3, 4
Oporto	40.14	71.99	Hot springs temperature 60 °C	3, 4
Cupido	40.15	71.91	Hot springs temperature 80 °C	3, 4
Chihuió	40.19	71.93	Hot springs temperature 82 °C	3, 4, 5
La Esperanza	40.34	71.82	Hot springs temperature 60 °C	3, 4
Puyehue	40.71	72.32	Hot springs temperature 75 °C	3, 4, 5
Rupanco	40.86	72.22	Hot springs temperature 63 °C	3, 4, 5
El Callao	40.98	72.16	Hot springs temperature 59 °C	3, 4
Las Juntas	41.25	72.04	Hot springs temperature 73 °C	3, 4
Cayetué	41.30	72.20	Hot springs temperature 65 °C	3, 4
Cochamó	41.36	72.32	Hot springs temperature 70 °C	3
Llancahue	42.07	72.51	Hot springs temperature 52 °C	3
Cahuelmó	42.26	72.38	Hot springs temperature 84 °C	2, 3
Michinmahuida	42.96	72.39	Hot springs temperature 65 °C	2, 3
Río Frio	43.47	72.47	Hot springs temperature 70 °C	2, 3
Puerto Bonito	43.95	72.73	Hot springs temperature 70 °C	2, 3
Puyuhapi	44.41	72.64	Hot springs temperature 80 °C	2, 3
Puerto Peréz	45.24	70.21	Hot springs temperature 90 °C	2, 3
Aguas Calientes	45.42	73.03	Hot springs temperature 65 °C	2, 3, 5
Contreras	45.44	73.11	Hot springs temperature 68 °C	2, 3
Quitralco	45.58	73.38	Hot springs temperature 65 °C	2, 3
Estero Negro	45.69	72.33	Hot springs temperature 60 °C	3
Huemules	45.87	73.29	Hot springs temperature 60 °C	3
Cupquelán	45.96	73.39	Hot springs temperature 60 °C	3
Huiña	46.31	72.81	Hot springs temperature 55 °C	3
Caleta Román	46.06	75.51	Hot springs temperature 65 °C	3

and structural setting points to a N-S elongated shape for the reservoir ([García, 2014](#)). Geothermometers must be used with extreme caution due to probable salt contamination ([Risacher et al., 2011](#)).

#### Sierra Nevada geothermal area

The Sierra Nevada geothermal system is associated with the similarly named Pleistocene-Holocene volcano in the Araucanía region of Chile. There are surface manifestations extending on the N and NW flanks of the volcano. Gas compositions of fumaroles suggest a high enthalpy, liquid dominated reservoir with an equilibrium temperature of ~215 °C ([Muñoz et al., 2011](#)). Further geophysical studies are essential to constrain the depth and dimensions of the inferred geothermal reservoir.

#### 4.3. Interest areas

Based on geothermal exploration at a regional scale ([Días, 1983](#); [Hauser, 1989, 1997](#); [Peréz, 1999](#); [Risacher et al., 2011](#)) and surface geothermal features, the interest areas are summarized in [Table 4](#).

#### 5. Discussion

The experience of recent decades has shown that the Heat in Place method is usually biased high. The tendency to overestimate the potential of geothermal prospects, in particular, has led to the reduced credibility of the method ([Grant, 2015](#)). Much of the

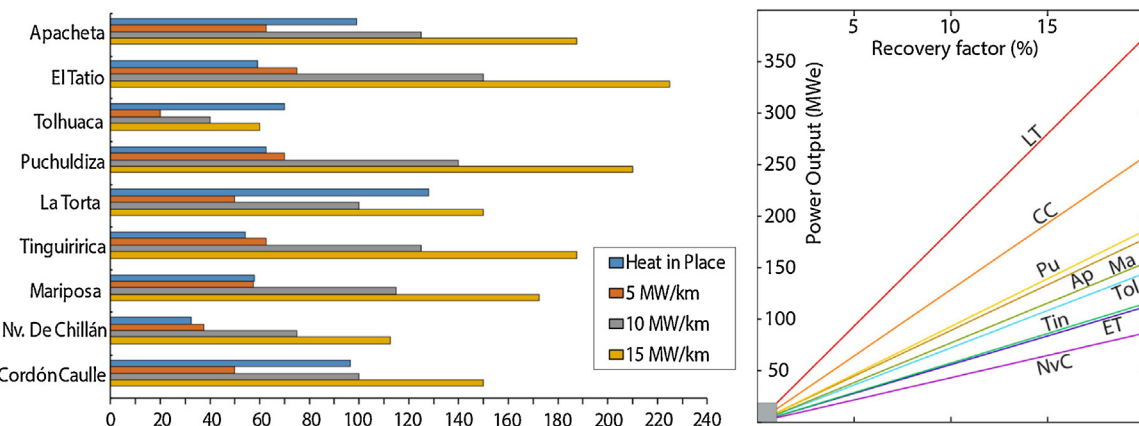


**Fig. 7.** Left: Tornado diagram comparing results of this work with the power density method applied to the half of the areal extent of conductive anomaly. Right: Recovery factor sensitivity test for each system.

problem lies in the estimation of the recovery factor, the proportion of the resource that can actually be exploited. This factor cannot be determined without further evaluation of the reservoir's structural control and permeability heterogeneity (López and Smith, 1996; Rowland and Sibson, 2004). For low permeability systems (such as EGS), this recovery factor may be less than 0.02 (Grant and Garg, 2012; Grant, 2015). Wilmarth and Stimac (2015) estimated the power densities of 66 geothermal fields above 10 MW<sub>net</sub> with more than 5 years of production history. Their work suggests that volcanic arc systems tend to be moderate to high-temperature and have moderate to high power densities (5–15 MWe/km<sup>2</sup>). Wilmarth and Stimac (2015), and references therein, state that the fraction of the geothermal anomaly determined from low resistivity and thermal area that may eventually be developed is typically on the order of 0.5, but may range from 0 to more than 1. In this work we apply the power density method to an areal extent corresponding to half of the conductive anomaly. Fig. 7 (Left) depicts a comparison with results after applying the power density method to each system. Values obtained in Apacheta, La Torta, Tolhuaca, and Cordón Caulle correlate with a power density equivalent of ~8–15 MWe/km<sup>2</sup>; the remaining systems correlate nicely within a range of 4–5 MWe/km<sup>2</sup> suggesting that Andean systems might hold a much higher power potential if a best case scenario is achieved. Although the volume method provides a means of estimating the heat content of a geothermal reservoir, it does not explicitly predict the reservoir permeability (Williams et al., 2008). The structural setting in the Chilean volcanic arc is dominantly compressive (Fig. 1), but with varying complexities regarding each system's local context. This variability is a source of uncertainty that must be taken into account. Puchuldiza, Apacheta, El Tatio/La Torta and Cordón Caulle are graben-related geothermal areas near an active volcanic arc. These systems show extensive superficial features, suggesting the occurrence of medium to high permeability. On the other hand, volcanic-related systems like Tinguiririca, Mariposa, Nevados de Chillán and Tolhuaca are highly influenced by episodic re-shearing events. The nature of permeability in these areas is still a matter of debate. Further studies regarding permeability in Andean systems is highly recommended in order to understand its influence on the recovery factor.

Published data from 94 geothermal plants (Zarrouk and Moon, 2014) helps to constrain single flash plant efficiency, and new models for the recovery of heat from heterogeneous, fractured reservoirs (Williams et al., 2008) provide a physically realistic basis for evaluating the production potential of natural geothermal reservoirs. Calculations are based upon recovery and conversion factors from single flash and dry steam power plants (Zarrouk and Moon,

2014), since this is the type of power plant installed at a newly developed high temperature geothermal fields (>200). Once the single flash steam power plant is running, DiPippo (2012a) recommends the installation of a double flash steam power plant in order to produce 15–25% more power output for the same geothermal fluid conditions. Many plants often include both flash and binary systems to maximize electrical power generation. Nevertheless, an economic analysis is required for each individual system in order to properly address this issue.

Apacheta, La Torta, Tinguiririca, and Mariposa encompass extensive superficial features, suggesting the presence of large systems. Estimated volume and temperature of these areas show a high variability. For large geothermal systems, variation of temperature causes a great uncertainty in available energy. As a result, estimated power output for large systems show a higher standard deviation (Table 2).

The electrical anomaly, recorded by MT or TEM surveys, is usually interpreted as a result of successive alteration processes, which are part of the geothermal system evolution. Those processes can migrate over time. Therefore, the areal extent of the geothermal system inferred from the dimension of the clay cap may be overestimated, because there are no guarantees of geothermal fluid below the clay cap (e.g., the clay cap could correspond to a fossil system).

Temperature estimation can be a major source of uncertainty. If the up-flow zone has not been reached by exploratory wells, there is a chance temperatures can be underestimated. On the other hand, the application of geothermometers can lead to gross overestimation if they are not interpreted with caution.

Indicated and Inferred systems can be grossly classified into high and medium potential power-producing systems. Apacheta, La Torta and Cordón Caulle yield values of 99, 128 and 97 MWe respectively. The remaining systems (Nv. de Chillán, Tinguiririca, Mariposa, El Tatio and Tolhuaca in increasing order) range from 32 to 70 MWe, consistent with mean production values for volcanic-hosted geothermal systems (e.g. Zarrouk and Moon, 2014 and references therein).

The heat source in El Tatio/La Torta and Puchuldiza remains unclear. It is necessary to consider the combined influence of volcanic convection-dominated systems (Moeck, 2014), yet with a high influence of a regional heat flow anomaly. Geophysical surveys in El Tatio and La Torta suggests both systems share the same deep geothermal reservoir (Cumming et al., 2002), and are the largest Inferred system in the Chilean Andes, yielding 187 MWe with a standard deviation of 121 MWe. Additionally, the Sol de la Mañana geothermal field lies just 20 km east, on the east edge of the Pre-Altiplanic Cordillera, supporting the hypothesis of deep, high

temperature reservoirs emplaced along this segment of the arc. Deep drilling and an EGS approach can be assessed as an alternative for several mining projects located along the CVZ whose energetic needs are consistent with geothermal high plant factors.

Many Andean systems present fluids of an acid nature which can be problematic due to the impact in costs and maintenance. Nevertheless, the resource can be exploited by binary plants (DiPippo, 2008). Therefore, despite there is no consideration about geothermal fluid composition, the geothermal power potential is still valid even in the case of problematic geothermal fluids.

## 6. Conclusion

We gathered and ranked geothermal exploration data available in the literature, establishing categories of Measured, Indicated, and Inferred geothermal resource. We then applied numerical methods to 9 high enthalpy reservoirs ( $>200^{\circ}\text{C}$ ) in the Chilean Andes. In addition, 8 areas are highlighted as highly favorable, based on geological, geochemical and/or geophysical surveys. Furthermore, 57 geothermal areas are considered as potential high enthalpy geothermal resources, suggesting there are many undiscovered geothermal systems in the Chilean Andes.

Based on available published geological, geochemical and geophysical evidence, the total Indicated resource is 228 MWe with a standard deviation of 119 MWe. Inferred resources reach 431 MWe with a standard deviation of 321 MWe, adding up to 659 MWe among medium (6) and large (3) systems in the Chilean Andes. This total estimated power potential is equivalent to  $\sim 4.4\%$  of the total installed electric capacity in Chile.

Although volumetric methods provide a means of estimating the heat content of a geothermal reservoir, it does not explicitly predict the power potential. It does allow for a gross estimate and a comparative evaluation of the different geothermal prospects. Comparison with values obtained through the power density method leads to a better understanding of the full uncertainty of resource capacities.

Despite the high degree of geologic uncertainty, finite element modeling is highly recommended for Indicated and Inferred systems (Table 2). This approach provides a more rigorous way to evaluate and understand conceptual models and system thermodynamics.

## Acknowledgments

This work has been supported by the FONDAP/CONICYT Project number 15090013 (Centro de Excelencia en Geotermia de los Andes, CEGA) and Departamento de Geología, FCFM, Universidad de Chile. P. Dobson was supported by Lawrence Berkeley National Laboratory under U.S. Department of Energy, Assistant Secretary for Energy Efficiency and Renewable Energy, Geothermal Technologies Office, under the U.S. Department of Energy Contract no. DE-AC02-05CH11231. The authors would especially like to thank Dra. Jennifer Blank and two anonymous reviewers for their valuable comments.

## References

- Achurra, L., 2011. Estudio hidrogeoquímico sobre la interacción de aguas subterráneas profundas y someras en Pampa Lirima, Norte de Chile. Universitat Politècnica de Catalunya Barcelona (Master thesis).
- Aguirre, I., Clavero, J., Simmons, S., Giavelli, A., Mayorga, C., Sofía, J., 2011. Colpitas – a new geothermal project in Chile. Geothermal Resources Council Transactions, vol. 35. California, pp. 1141–1145.
- Aldrich, M., Laughlin, A., Gambill, D., 1981. Geothermal Resource Base of the World: A Revision of the Electrical Power Research Institute's Estimate. Technical Report Electrical Power Research Institute.
- Aravena, D., Lahsen, A., 2012. Assessment of exploitable geothermal resources using magmatic heat transfer method, Maule Region, Southern Volcanic Zone, Chile. Geothermal Resources Council Transactions, vol. 36. California, pp. 1307–1313.
- Aravena, D., Lahsen, A., 2013. A geothermal favorability map of Chile, preliminary results. Geothermal Resources Council Transactions, vol. 37. Geothermal Resources Council, California.
- Arcos, R., Clavero, J., Giavelli, A., Simmons, S., Aguirre, I., Martini, S., Mayorga, C., Pineda, G., Parra, J., Sofía, J., 2011. Surface exploration at Pampa Lirima geothermal project, central Andes of northern Chile. Geothermal Resources Council Transactions, vol. 35. California, pp. 689–693.
- Capaccioni, B., Aguilera, F., Tassi, F., Darrah, T., Poreda, R., Vaselli, O., 2011. Geochemical and isotopic evidences of magmatic inputs in the hydrothermal reservoir feeding the fumarolic discharges of Tacora volcano (northern Chile). J. Volcanol. Geotherm. Res. 208, 77–85, <http://dx.doi.org/10.1016/j.jvolgeores.2011.09.015> <http://www.sciencedirect.com/science/article/pii/S0377027311002587>.
- Cembrano, J., Lara, L., 2009. The link between volcanism and tectonics in the southern volcanic zone of the Chilean Andes: a review. Tectonophysics 471, 96–113, <http://dx.doi.org/10.1016/j.tecto.2009.02.038> <http://www.sciencedirect.com/science/article/pii/S0040195109001310>, Understanding stress and deformation in active volcanoes.
- Cembrano, J., Lavenu, A., Yañez, G.Y., Riquelme, R., García, M., Héral, G., González, G., 2007. Neotectonics. In: Moreno, T., Gibbons, W. (Eds.), *The Geology of Chile*. The Geological Society of London, London.
- Clavero, J., Pineda, G., Mayorga, C., Giavelli, A., Aguirre, I., Simmons, S., Martini, S., Sofía, J., Arriaza, R., Polanco, E., Achurra, L., 2011. Geological, geochemical, geophysical and first drilling data from Tingüiririca geothermal area, central Chile. Geothermal Resources Council Transactions, vol. 35. Geothermal Resources Council, California, pp. 731–734.
- Cumming, W., Vieytes, H., Ramirez, C., Sussman, D., 2002. Exploration of the La Torta geothermal prospect, northern Chile. In: Geothermal Resources Council Transactions, vol. 26. California, pp. 3–7.
- Cusicanqui, H., 1979. Estudio geoquímico del área termal de Surire – provincia de Arica – I Región, Technical Report Comité Geotérmico CORFO Santiago.
- De Silva, S., Francis, P., 1991. Volcanoes of the Central Andes. Springer-Verlag, Berlin.
- Días, F., 1983. Present state of geothermal research and development in Chile, Technical Report Servicio Nacional de Geología y Minería Santiago.
- DiPippo, R., 2008. Binary cycle power plants. In: DiPippo, R. (Ed.), *Geothermal Power Plants* (Second Edition), second ed. Butterworth-Heinemann, Oxford, pp. 157–189, <http://dx.doi.org/10.1016/B978-075068620-4.50013-7> <http://www.sciencedirect.com/science/article/pii/B9780750686204500137>, (chapter 8).
- DiPippo, R., 2012a. Geothermal power generating systems. In: DiPippo, R. (Ed.), *Geothermal Power Plants*, third ed. Butterworth-Heinemann, Boston, pp. 79–80, <http://dx.doi.org/10.1016/B978-0-08-098206-9.00032-4> <http://www.sciencedirect.com/science/article/pii/B9780080982069000324>, (chapter 2).
- DiPippo, R., 2012b. Reservoir engineering. In: DiPippo, R. (Ed.), *Geothermal Power Plants*, third ed. Butterworth-Heinemann, Boston, pp. 49–77, <http://dx.doi.org/10.1016/B978-0-08-098206-9.00004-X> <http://www.sciencedirect.com/science/article/pii/B978008098206900004X>, (chapter 4).
- Emparán, C., Suárez, M., Muñoz, J., 1997. Hoja Curacautín: Regiones de la Araucanía y del Biobío. Number 71 in *Carta Geológica de Chile*. Servicio Nacional de Geología y Minería, Santiago, 105 p. – 1 map.
- ENEL, 2012. Cerro Pabellón Geothermal Project (Apacheta), Technical Report Enel, Latinoamérica (Chile) Ltda.
- ENG, 2007. Estudio de impacto ambiental: Exploración geotérmica profunda Nevados de Chillán sector Valle de las Nieblas, Technical Report Empresa Nacional de Geotermia S.A.
- García, K., 2014. Aplicación del método magnetotelúrico en la exploración de un sistema geotermal, en la región de Atacama, Chile. Universidad de Chile, Santiago (Master's thesis), <http://tesis.uchile.cl/handle/2250/116320>.
- Garg, S.K., Combs, J., 2010. Appropriate use of USGS volumetric “heat in place” method and Monte Carlo calculations. In: Proceedings, 34th Workshop on Geothermal Reservoir Engineering. Stanford University, Stanford, CA, p. 7.
- Garg, S.K., Combs, J., 2015. A reformulation of USGS volumetric “heat in place” resource estimation method. Geothermics 55, 150–158, <http://dx.doi.org/10.1016/j.geothermics.2015.02.004> <http://www.sciencedirect.com/science/article/pii/S0375650515000280>.
- González-Ferrán, O., 1995. Volcanes de Chile, first ed. Instituto Geográfico Militar, Santiago.
- Grant, M., 2015. Resource assessment, a review, with reference to the Australian Code. In: Proceedings World Geothermal Congress, Melbourne.
- Grant, M., Garg, S., 2012. Recovery factor for EGS. In: Proceedings 37th Workshop on Geothermal Reservoir Engineering, 2012, Stanford University, Stanford, California.
- Hauser, A., 1989. Fuentes termales y minerales en torno a la Carretera Austral, regiones X-XI, Chile. Andean Geol. 16, 229–239.
- Hauser, A., 1997. Catastro y caracterización de las fuentes de aguas minerales termales de Chile. 50. Servicio Nacional de Geología y Minería, Santiago.
- Hickson, C., Ferraris, F., Rodriguez, C., Sielfeld, G., Henriquez, R., Gislason, T., Selters, J., Benoit, D., White, P., Southon, J., Ussher, G., Charroy, J., Smith, A., Lovelock, B., Lawless, J., Quinliven, P., Smith, L., Yehia, R., 2011. The Mariposa geothermal system, Chile. Geothermal Resources Council Transactions, vol. 35. California, pp. 817–825.
- Iriarte, S., Jornada Geotérmica Universidad de Concepción, 2013. Exploración geotérmica proyecto Tolhuaca.

- JICA, 1979. Informe preliminar segunda fase JICA – Proyecto de desarrollo del campo geotérmico de Puchuldiza. Technical Report Comité Geotérmico CORFO Santiago.
- Lahsen, A., 1976. Geothermal exploration in Northern Chile – summary. In: Circum-Pacific Energy and Mineral Resources. The American Association of petroleum Geologists, pp. 169–175.
- Lahsen, A., 1978. Evaluación de los resultados de la exploración del campo geotérmico de Puchuldiza I Región Tarapacá, Technical Report Comité Geotérmico CORFO, Santiago.
- Lahsen, A., 1986. Origen y potencial de energía geotérmica en los Andes de Chile, Technical Report Geología y Recursos Minerales de Chile, Universidad de Concepción Concepción.
- Lahsen, A., 1988. Chilean geothermal resources and their possible utilization. Geothermics 17, 401–410, [http://dx.doi.org/10.1016/0375-6505\(88\)90068-5](http://dx.doi.org/10.1016/0375-6505(88)90068-5).
- Lahsen, A., Muñoz, N., Parada, M.A., 2010. Geothermal development in Chile. In: World Geothermal Congress, Bali, pp. 25–29.
- Lahsen, A., Trujillo, P., 1976. El campo geotérmico de El Tatio, Chile. Proyecto Geotérmico CORFO-ONU, Technical Report Corporación de Fomento de la Producción (CORFO), Santiago.
- Lee, S., Simkin, T., Kimberly, P., 2010. Volcanoes of the World, 3rd ed. University of California Press, Berkeley and Los Angeles, CA.
- Legault, J., Lombardo, S., Zhao, S., Clavero, J., Aguirre, I., Arcos, R., Lira, E., 2012. ZTEM airborne AFMAG EM and ground geophysical survey comparisons over the Pampa Lirima geothermal field in northern Chile – a) Z-axis tipper electromagnetic system. Geothermal Resources Council Transactions, vol. 36. California, pp. 1001–1008.
- Letelier, M., 1981. Geoquímica de las manifestaciones termales de Puchuldiza y sus alrededores, Technical Report Comité Geotérmico CORFO, Santiago.
- Lira, E., 2011. Estudio de sismicidad, tomografía sísmica y modelo de física de rocas: Potencial sistema geotermal asociado al complejo volcánico Tinguiririca. Universidad de Chile, Santiago (Master's thesis).
- López, D.L., Smith, L., 1996. Fluid flow in fault zones: influence of hydraulic anisotropy and heterogeneity on the fluid flow and heat transfer regime. Water Resour. Res. 32, 3227–3235, <http://dx.doi.org/10.1029/96WR02101>.
- Lovekin, J., 2004. Geothermal inventory. Bull. Geotherm. Resour. Council 33, 242–244.
- Melosh, G., Moore, J., Stacey, R., 2012. Natural reservoir evolution in the Tolhuaca geothermal field, southern Chile. In: Proceedings 36th Workshop on Geothermal Reservoir Engineering, Stanford University, Stanford, CA.
- Moeck, I.S., 2014. Catalog of geothermal play types based on geologic controls. Renew. Sustain. Energy Rev. 37, 867–882, <http://dx.doi.org/10.1016/j.rser.2014.05.032> <http://www.sciencedirect.com/science/article/pii/S1364032114003578>.
- Moreno, H., Gardeweg, M., 1989. La erupción reciente en el Complejo Volcánico Lonquimay (diciembre 1988). Andes del Sur. Andean Geol. 16, 93–117.
- Muffler, L., 1979. Assessment of geothermal resources of the United States – 1978, Circular 790, U.S. Geological Survey.
- Muffler, L., Cataldi, M., 1978. Assessment of geothermal resources of the United States – 1978. In: Muffler, L. (Ed.), Geological Survey Circular 790. U.S. Geological Survey, Arlington, pp. 1–7.
- Muñoz, J., Stern, C., 1988. The Quaternary volcanic belt of the southern continental margin of South America: transverse structural and petrochemical variations across the belt between 38°S and 39°S. J. S. Am. Earth Sci. 1, 147–161, [http://dx.doi.org/10.1016/0895-9811\(88\)90032-6](http://dx.doi.org/10.1016/0895-9811(88)90032-6) <http://www.sciencedirect.com/science/article/pii/0895981188900326>.
- Muñoz, M., Alam, A., Parada, M., Lahsen, A., 2011. Geothermal system associated with the Sierra Nevada volcano, Araucanía region, Chile. Geothermal Resources Council Transactions, vol. 35. California, pp. 935–941.
- Nathenson, M., 1975. Physical factors determining the fraction of stored energy recoverable from hydrothermal convection systems and conduction-dominated areas. Open-File Report 75-525. U.S. Geological Survey.
- Ortiz, M., Achurra, L., Cortés, R., Fonseca, A., Silva, C., Vivallos, J., 2008. Estudio geológico, geofísico e hidroquímico del sector Puchuldiza sur. Servicio Nacional de Geología y Minería, Santiago (Unpublished report), 1 map.
- Pérez, P., Sánchez, P., Arancibia, G., Cembrano, J., Veloso, E., Lohmar, S., Stimac, J., Reich, M., Rubilar, J., 2012. Sampling and detailed structural mapping of veins, fault-veins and faults from Tolhuaca Geothermal System, southern Chile. Congreso Geológico Chileno. Antofagasta, vol. 13.
- Peréz, Y., 1999. Fuente de aguas termales de la Cordillera Andina del centro-sur de Chile (39–42°S, 54. Servicio Nacional de Geología y Minería, Santiago, 1 map 1:500,000.
- Procesi, M., 2014. Geothermal potential evaluation for northern Chile and suggestions for new energy plans. Energies 7, 5444–5459, <http://dx.doi.org/10.3390/en7085444> <http://www.mdpi.com/1996-1073/7/8/5444>.
- Ramírez, C., Huete, C., 1981. Hoja Ollague, escala 1:250,000. Carta Geológica de Chile, Servicio Nacional de Geología y Minería, Santiago, 47 p. – 1 map.
- Reyes, N., Vidal, A., Ramírez, E., Arnason, K., Richter, B., Steingrimsson, B., Acosta, O., Camacho, J., 2011. Geothermal exploration at Irruputuncu and Olca volcanoes: pursuing a sustainable mining development in Chile. Geothermal Resources Council Transactions, vol. 35. California, pp. 983–986.
- Risacher, F., Fritz, B., Hauser, A., 2011. Origin of components in Chilean thermal waters. J. S. Am. Earth Sci. 31, 153–170, <http://dx.doi.org/10.1016/j.james.2010.07.002> <http://www.sciencedirect.com/science/article/pii/S0895981110000349>.
- Rojas, E., Folguera, A., Zamora, G., Bottesi, G., Ramos, V., 2014. Structure and development of the Andean system between 36°S and 39°S. J. Geodyn. 73, 34–52, <http://dx.doi.org/10.1016/j.jog.2013.09.001> <http://www.sciencedirect.com/science/article/pii/S0264370713001336>.
- Rojas, G., 2013. Magnetotellurica en el Complejo Volcánico Cordón Caulle. Universidad de Concepción (Bachelor thesis).
- Rosenau, M., Melnick, D., Echtler, H., 2006. Kinematic constraints on intra-arc shear and strain partitioning in the southern Andes between 38°S and 42°S latitude. Tectonics 25, <http://dx.doi.org/10.1029/2005TC001943>.
- Rowland, J., Sibson, R., 2004. Structural controls on hydrothermal flow in a segmented rift system, Taupo Volcanic Zone, New Zealand. Geofluids 4, 259–283, <http://dx.doi.org/10.1111/j.1468-8123.2004.00091.x>.
- Sánchez, P., Morata, D., Lahsen, A., Aravena, D., Parada, M.A., 2011. Current status of geothermal exploration in Chile and the role of the new Andean Geothermal Center of Excellence (CEGA). Geothermal Resources Council Transactions, vol. 35. California, pp. 1215–1218.
- Sarmiento, Z., Ármanansson, H., Abanes, R., Marangunic, C., Ingimundarson, A., O'Ryan, R., 2010. Revisión de la ejecución del proyecto Perforación Geotérmica Profunda El Tatio, Fase I, Informe Final, Technical Report Comisión Nacional de Energía, Chile.
- Sepúlveda, F., 2005. El sistema Geotérmico de Cordón Caulle: caracterización geológica y geoquímica. Universidad de Chile (Ph.D. thesis).
- Sepúlveda, F., Lahsen, A., 2003. Geothermal exploration in central-southern Chile (33–42°S). Geothermal Resources Council Transactions, vol. 27, pp. 635–638.
- Sepúlveda, F., Lahsen, A., Powell, T., 2007. Gas geochemistry of the Cordón Caulle geothermal system, southern Chile. Geothermics 36, 389–420, <http://dx.doi.org/10.1016/j.geothermics.2007.05.001> <http://www.sciencedirect.com/science/article/pii/S0375650507000533>.
- SERNAGEOMIN, 2003. Mapa geológico de Chile: versión digital. Digital Geological Publishing, No. 4 (CD-ROM, version 1.0, 2003).
- Tassi, Aguilera, F., Darrah, T., Vaselli, O., Capaccioni, B., Poreda, R., Huertas, A.D., 2010. Fluid geochemistry of hydrothermal systems in the Arica-Parinacota, Tarapacá and Antofagasta regions (northern Chile). J. Volcanol. Geotherm. Res. 192, 1–15, <http://dx.doi.org/10.1016/j.jvolgeores.2010.02.006> <http://www.sciencedirect.com/science/article/pii/S0377027310000405>.
- Tassi, F., Aguilera, F., Vaselli, O., Darrah, T., Medina, E., 2011. Gas discharges from four remote volcanoes in northern Chile (Putana, Olca, Irruputuncu and Alitar): a geochemical survey. Ann. Geophys. 54, <http://dx.doi.org/10.4401/ag-5173> <http://www.annalsofgeophysics.eu/index.php/annals/article/view/5173>.
- Tassi, F., Martínez, C., Vaselli, O., Capaccioni, B., Viramonte, J., 2005. Light hydrocarbons as redox and temperature indicators in the geothermal field of El Tatio (northern Chile). Appl. Geochem. 20, 2049–2062, <http://dx.doi.org/10.1016/j.apgeochem.2005.07.013> <http://www.sciencedirect.com/science/article/pii/S0883292705001599>.
- Tebbens, S., Cande, S., Kovacs, L., Parra, J., LaBrecque, J., Vergara, H., 1997. The Chile ridge: a tectonic framework. J. Geophys. Res.: Solid Earth (1978–2012) 102, 12035–12059, <http://dx.doi.org/10.1029/96BO2581>.
- Tocchi, E., 1923. Il Tatio, ufficio geológico Larderello SpA (Unpublished report).
- Urzúa, L., Powell, T., Cumming, W., Dobson, P., 2002. Apacheta, a new geothermal prospect in northern Chile. Geothermal Resources Council Transactions, vol. 26, pp. 65–69.
- Vázquez, M., Nieto, F., Morata, D., Drogue, B., Carrillo-Rosua, F., Morales, S., 2014. Evolution of clay mineral assemblages in the Tinguiririca geothermal field, Andean Cordillera of central Chile: an {XRD} and HRTEM-AEM study. J. Volcanol. Geotherm. Res. 282, 43–59, <http://dx.doi.org/10.1016/j.jvolgeores.2014.05.022> <http://www.sciencedirect.com/science/article/pii/S0377027314001760>.
- White, D., Williams, D., 1975. Assessment of geothermal resources of the United States – 1975, Circular 726 U.S. Geological Survey.
- Williams, C., Reed, M., Mariner, R., 2008. A review of methods applied by the US Geological Survey in the assessment of identified geothermal resources, Open-File Report 2008-1296, U.S. Geological Survey.
- Wilmarth, M., Stimac, J., 2015. Power density in geothermal fields. In: Proceedings World Geothermal Congress, Melbourne.
- Zarrouk, S.J., Moon, H., 2014. Efficiency of geothermal power plants: a worldwide review. Geothermics 51, 142–153, <http://dx.doi.org/10.1016/j.geothermics.2013.11.001> <http://www.sciencedirect.com/science/article/pii/S0375650513001120>.